Bispecific Antibody Pretargeting of Tumor Neovasculature for Improved Systemic Radiotherapy of Solid Tumors

Dieter Moosmayer,[1] Dietmar Berndorff,[1] Chien-Hsing Chang,[2] Robert M. Sharkey,[5] Axel Rother,[4] Sandra Borkowski,[1] Edmund A. Rossi,[2] William J. McBride,[3] Thomas M. Cardillo,[3] David M. Goldenberg,[5] and Ludger M. Dinkelborg[1]

Abstract

Purpose: Extra domain B (ED-B) fibronectin is a specific tumor matrix marker for targeting angiogenesis in solid tumors. In this study, the radiotherapeutic potential of the directly radioiodinated divalent anti-ED-B antibody fragment, L19 small immunoprotein (L19-SIP; 75,000 Da), was compared with a pretargeting approach using the bispecific antibody AP39xm679 (bsMAb; 75,000 Da).

Experimental Design: The bsMAb was prepared by coupling an anti-ED-B single-chain Fv (AP39) to the Fab′ of the murine antibody m679, which binds to the small peptidic hapten histamine-succinyl-glycine (HSG). As an effector molecule for the pretargeting approach, the ^{111}In-labeled HSG-DOTA complex was injected 25 or 41 hours after the bsMAb. The kinetics of both the iodinated bsMAb and the pretargeted ^{111}In-labeled HSG hapten were investigated in mice bearing human glioblastoma xenografts (U251) and compared with the kinetics and tumor accumulation of radioiodinated L19-SIP. ^{111}In and ^{125}I were used as surrogate marker for the therapeutic radioisotopes ^{90}Y/^{177}Lu and ^{131}I, respectively.

Results: Tumor uptake of the pretargeted ^{111}In-labeled peptide was significantly higher than ^{125}I-L19-SIP over 7 days. At the calculated maximally tolerated dose for each agent (with the kidney being the dose-limiting organ for pretargeting and the bone marrow for direct targeting), a mouse tumor dose of 146 Gy could be given by pretargeting versus 45 Gy delivered by the direct approach.

Conclusions: These data suggest that pretargeting of ED-B with AP39xm679 and subsequent injection of the ^{90}Y-hapten-peptide would improve the therapeutic efficacy in solid tumors by >3-fold compared with directly radiolabeled ^{131}I-L19-SIP.

Radioimmunotherapy, the systemic administration of radioisotope-labeled tumor-targeting monoclonal antibodies (MAb), has been successful as a treatment for certain types of non–Hodgkin's lymphoma but has had little success in the treatment of most solid tumors (1). This is due to the fact that, at maximally tolerated doses, radioimmunotherapy is not able to deliver a sufficiently high enough radiation dose to have a significant effect on the growth of solid tumors especially when applied as a monotherapy. In radioimmunotherapy, the hematologic toxicity caused by the high and long-lasting blood activities of MAbs is dose limiting. This is due to the continuous source of radiation to the highly radiosensitive red marrow. To overcome this limitation of directly radiolabeled IgG MAbs, enzymatic fragmentation or genetic engineering has been used to create constructs that clear rapidly from the blood and achieve maximum tumor accumulation more rapidly than a full-size MAb. Although the tumor-to-blood ratios can be improved significantly with these constructs because of their faster clearance from the blood, both the total amount of radioactivity delivered to the tumor as well as the tumor residence time are decreased (2). Thus, the advantage of being able to administer higher activities is offset by a decreased total tumor dose. This is especially true when MAbs, fragments thereof, are radiolabeled with radiometals or lanthanides because the bifunctional chelators needed for labeling become trapped in the proximal tubules of the kidney, leading to unwanted and high radiation doses to this organ that often are higher or equal to the tumor doses achieved (3).

One approach to overcome the limitations posed by direct radiolabeling of MAbs or their smaller fragments/constructs is the use of pretargeting (4, 5). The pretargeting systems solve the slow blood clearance problem by attaching the radionuclide to a very small compound that is characterized by rapid body elimination via renal clearance (~80% of the injected activity excreted in the urine within 1-2 hours in mice).

Authors' Affiliations: [1]Schering AG, Research Laboratories, Berlin, Germany; [2]IBC Pharmaceuticals, Inc.; [3]Immunomedics, Inc., Morris Plains, New Jersey; [4]Forschungszentrum Rossendorf eV, Institut für Bioorganische und Radiopharmazeutische Chemie, Dresden, Germany; and [5]Center for Molecular Medicine and Immunology, Belleville, New Jersey

Received 1/27/06; revised 5/3/06; accepted 7/6/06.

The costs of publication of this article were defrayed in part by the payment of page charges. This article must therefore be hereby marked *advertisement* in accordance with 18 U.S.C. Section 1734 solely to indicate this fact.

Note: D. Moosmayer and D. Berndorff contributed equally to this work.

Requests for reprints: Dieter Moosmayer, Schering AG Research Laboratories, Protein Chemistry, Muellerstrasse 178, 13342 Berlin, Germany. Phone: 49-30-468-17038; Fax: 49-30-468-16707; E-mail: dieter.moosmayer@schering.de.

©2006 American Association for Cancer Research.

doi:10.1158/1078-0432.CCR-06-0210

Downloaded from http://aacrjournals.org/clincancerres/article-pdf/12/18/5587/1966519/5587.pdf by guest on 10 November 2024

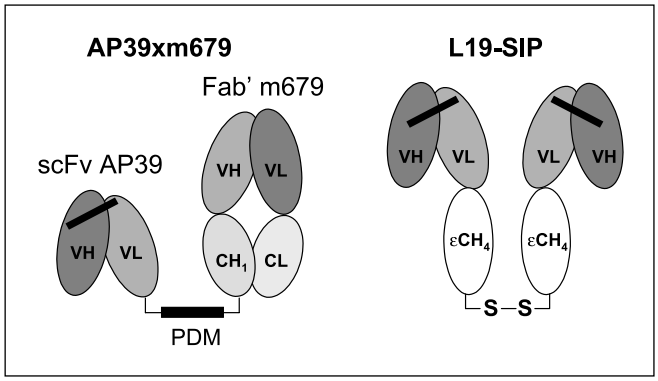

Fig. 1. Schematic drawing of the applied MAb constructs bsMAb AP39xm679 and L19-SIP. In the bsMAb AP39xm679, the scFv AP39 (which encodes a tag with an unpaired cysteine) is cross-linked via PDM to the Fab′ 679. In the SIP molecule, the dimerization of V_L and V_H domains of L19 scFv is achieved by recombinant connection of the L19 scFv to the C_H4 domain of the human IgE secretory isoform IgE-S2.

Moreover, these small molecules are able to quickly extravasate and diffuse to their tumor targets very efficiently. Because of their rapid diffusion and kidney elimination, these small molecules need to be very tumor selective and their specific targeting needs to occur with a high affinity, which can be achieved, for example, by making use of biotin/avidin binding, hapten/antibody binding, or the complementary oligonucleotide recognition systems (6). In this study, we used a bispecific Mab (bsMAb), consisting of one binding moiety specific for the angiogenesis-associated target, extra domain B (ED-B) fibronectin, and the other specific for a small hapten that can be radiolabeled either with ^{111}In or ^{90}Y after attachment of a bifunctional chelator. The unlabeled bsMAb is given first and allowed to accumulate in the tumor. Subsequently, the rapidly clearing radiolabeled hapten is injected. The interval between the bsMAb targeting and the subsequent injection of the radiolabeled compound is dependent on the blood clearance properties of the bsMAb and has to be optimized. If given too soon, a sizable fraction of the radiolabeled hapten-peptide binds to the bsMAb in the blood, slowing its clearance from the circulation. This type of pretargeting also benefits from the use of bivalent hapten-peptides, which greatly increase tumor uptake and retention, a mechanism known as the "affinity enhancement system" (7). High cure rates can be achieved by pretargeted radioimmunotherapy in mice bearing human colon carcinoma xenografts, significantly improving therapeutic responses if compared with directly radiolabeled IgG or F(ab′)$_2$ (8–13). In addition, Kraeber-Bodere et al. (14) have shown that repeated pretargeting applications increase the therapeutic efficacy without increasing its systemic toxicity in a human medullary thyroid cancer mouse model and that pretargeted radioimmunotherapy can be used with paclitaxel combination therapy to further improve efficacy in this animal model.

The fibronectin splice variant B (ED-B) is considered a pan-species angiogenesis-associated tumor matrix marker that is expressed in close proximity to the tumor neovasculature and in the stroma of a large variety of hyperplastic and neoplastic tissues. It is also expressed in healthy tissues during angiogenic processes (15). The completely human anti-ED-B single-chain Fv (scFv) MAb fragment L19 with a subnanomolar affinity has been generated (16). Derivatives of scFv L19 have been applied successfully in different strategies for tumor imaging and therapy in both animal models (17–19) as well as in patients for immunoscintigraphic detection of primary tumors and their metastases (20). ED-B is considered to be a promising target for radioimmunotherapy of solid tumors because, being a matrix antigen expressed in close vicinity of new tumor vessels, it is rapidly accessible via the circulation, and its relationship to the angiogenic processes in the tumor might facilitate selective destruction of tumor vasculature (21).

Berndorff et al. (21) recently examined three derivatives of the L19 anti-ED-B MAb (i.e., a 50,000-Da scFv, the 75,000-Da small immunoprotein (SIP), and the 150,000-Da IgG) radiolabeled with ^{90}Y or ^{131}I and determined that ^{131}I-L19-SIP had the most favorable biodistribution properties and superior antitumor effects compared with the other radiolabeled derivatives investigated. L19-SIP is a divalent scFv fusion protein encoding an IgE C_H4 domain for dimerization (21). To investigate the potential of the pretargeting system in combination with the ED-B tumor matrix marker, scFv AP39 (derived from scFv L19) was used to form a bsMAb with the murine anti-histamine-succinyl-glycine (HSG) 679 Fab′ (AP39xm679; Fig. 1). As a hapten, ^{111}In-labeled HSG was used. For subsequent *in vivo* characterization, the human glioblastoma xenograft model U251 was chosen. In this tumor model, ED-B expression can be detected in the perivascular space as well as in the stroma.[6] The kinetics of both the iodinated bsMAb as well as the ^{111}In-labeled HSG hapten were investigated in mice bearing human glioblastoma xenografts (U251) and compared with the kinetics and tumor accumulation of the radioiodinated L19-SIP.

Materials and Methods

Antibody derivatives. scFv AP39 was generated by insertion of the peptide sequence $(Gly)_3$-Cys-Ala at the COOH-terminal end of the V_L chain of the scFv L19. Expression in *Pichia pastoris* and product purification were done according to Cunha et al. (22). Briefly, the AP39-encoding DNA sequence was cloned into the *P. pastoris* expression vector pPIC9K (Invitrogen, Carlsbad, CA). This construct contains a methanol-inducible promoter (AOX1) and a signal sequence (from yeast α factor) for expression and secretion of the recombinant product. Stably transfected yeast clones (based on strain GS115) were established by electroporation and subsequent antibiotic selection. The clones were cultivated at 30°C in buffered minimal glycerol-complex medium or basal mineral medium, and methanol was added for promoter induction during the expression phase. The recombinant product had a correctly processed terminus and high antigen-binding activity. AP39 was purified from culture supernatant by protein A affinity chromatography and size exclusion chromatography followed by Tris (2-carboxy-ethyl)-phosphin-HCl treatment (for reduction of covalent dimers).

The purified AP39 forms a noncovalent dimeric scFv molecule (M_r ~50,000 Da). L19-SIP is a 75,000-Da SIP that was expressed in mammalian cells and purified by immunoaffinity chromatography as described earlier (23). Different L19-based MAb formats have been shown to have similar binding affinities when measured in solution to avoid avidity effects, but when the antigen is bound to a solid phase,

[6] Unpublished data.

Downloaded from http://aacrjournals.org/clincancerres/article-pdf/12/18/5587/1966519/5587.pdf by guest on 10 November 2024

these bivalent L19-based formats show better performance due to slow disassociation rates (24).

The murine anti-HSG IgG (m679) was purified from tissue culture medium by protein A and ion exchange chromatography. The $F(ab')_2$ was prepared by pepsin digestion. The AP39xm679 bsMAb was made by cross-linking reduced sulfhydryl groups with *N,N′*-1,2-phenylenedimaleimide (PDM; Aldrich, Milwaukee, WI). Briefly, AP39 and 679 $F(ab')_2$ were both reduced with 2 mmol/L Tris (2-carboxy-ethyl)-phosphin-HCl (Pierce, Rockford, IL) in 0.1 mol/L phosphate buffer (pH 7.4) for 30 minutes at 37°C. The reduced proteins (AP39-SH and 679 Fab′-SH) were dialyzed into coupling buffer [50 mmol/L sodium acetate, 0.5 mmol/L EDTA (pH 5.0)]. AP39-SH was then derivatized with a 500-fold molar excess of PDM by adding an aliquot of 20 mmol/L PDM (prepared in 90% *N,N′*-dimethylforamide) to a final concentration of 4 mmol/L. After 30 minutes at room temperature, the reaction mixture was dialyzed into coupling buffer to remove unreacted PDM. AP39-PDM was then combined with 679 Fab′-SH at a molar ratio of 1.5:1 and, after 90 minutes at room temperature, was quenched with 10 mmol/L cysteine. The solution was adjusted to pH 7.0 with Na_2HPO_4.

The resulting AP39xm679 Fab conjugate was purified using two affinity chromatography steps. Affinity chromatography with IMP-291-Affigel (25), which binds 679 MAb, removed unreacted AP39-PDM. The IMP-291-purified material was further purified using protein A agarose, which specifically binds AP39 but not 679 Fab′ and removes unreacted 679 Fab′. Purity of the material was determined by size exclusion high-pressure liquid chromatography (HPLC) and SDS-PAGE, whereas the bispecific binding of the AP39xm679 bsMAb was determined by BIAcore analysis.

Radiolabeling of antibodies and HSG-hapten-peptide. Radioiodination was done following a slightly modified version of the original Iodo-Gen method (26) using Iodo-Gen precoated iodination tubes (Pierce). Briefly, 200 μg (L19-SIP) or 280 μg (AP39xm679 bsMAb) of protein in 500 μL PBS were labeled with 0.5 mCi of Na ^{125}I (Amersham Biosciences, Little Chalfont, United Kingdom). After incubation at room temperature for 10 minutes, the radiolabeled protein was separated from free radioiodine by gel filtration using NAP5 columns (Amersham Biosciences, Upssala, Sweden) that were pretreated with 0.5% bovine serum albumin in PBS and equilibrated and eluted with PBS.

Each radiolabeled protein was tested for purity and immunoreactivity before its use. Size exclusion HPLC was done using a TSK-gel column SWxL, 300 × 7.8 mm (Tosoh Haas, Montgomeryville, PA), with TSK buffer (0.1 mol/L Na_2HPO_4, 0.1 mol/L Na_2SO_4, 0.05 mol/L NaN_3) as the mobile phase and a flow rate of 0.5 mL/min.

The immunoreactivity of the radioimmunoconjugates was determined using a test column composed of a Pasteur pipette filled with 250 μL ED-B Sepharose resin (27) and saturated with 0.5% bovine serum albumin in PBS. The test column was loaded with ~0.2 MBq radiolabeled protein in 500 μL of 0.5% bovine serum albumin in PBS and rinsed with 2 × 500 μL of 0.5% bovine serum albumin in PBS to remove the nonimmunoreactive fraction. The immunoreactive fraction was then eluted with 2 × 750 μL of aqueous triethylamine solution (0.1 mol/L). The radioactivity of the fractions and that remaining on the column was measured with a dose calibrator. The immunoreactive fraction was expressed as the percentage radioactivity bound to the column. After purification, the concentration of AP39xm679 bsMAb was determined by measurement of the absorbance of the sample with an UV spectrometer, and the specific activity needed for the biodistribution studies was adjusted by addition of nonlabeled protein.

The hapten-peptide used in these studies was the divalent HSG-1,4,7,10-tetra-azacylododecane *N,N′,N′,N′*-tetraacetic peptide IMP-241 (28) provided by Immunomedics, Inc. (Morris Plains, NJ). The hapten-peptide was dissolved in 0.5 mol/L ammonium acetate (pH 5.5) to a concentration of 2.0×10^{-3} mol/L and radiolabeled with $^{111}InCl_3$ (Amersham Health, Little Chalfont, United Kingdom) according to Sharkey et al. (28). Unbound ^{111}In was measured by instant TLC and done using a water-ethanol-ammonia mixture (5:2:1) as a mobile phase. Additionally, reversed-phase HPLC was done using a Zorbax Bonus-RP column, 250 × 6 mm (Tosoh Haas), with an acetonitrile plus 0.1% trifluoroacetic acid/water plus 0.1% trifluoroacetic acid gradient (0-45% organic phase in 15 minutes) and a flow rate of 1.5 mL/min. The ^{111}In-labeled hapten-peptide solution was used for the biodistribution studies without further purification.

Animals. Female nude mice (NMRI-Foxn1^{nu}) were obtained from Taconic Europe (Bomholtgard, Denmark), and tumors were induced by inoculation of 2.2×10^6 human glioblastoma (U251) cells s.c. into the right hind limb. Biodistribution experiments were carried out after 20 to 28 days when tumors reached a mass of 50 to 300 mg. All animal experiments were done in compliance with the German law on the protection of animals.

Biodistribution studies. Biodistributions of nonpretargeted ^{125}I-labeled bsMAb (~1.1 μg, 61 kBq) and ^{125}I-L19-SIP (~0.45 μg, 48.5 kBq) were obtained at the indicated time points after i.v. injection of the radiolabeled MAb in a total volume of 0.1 mL. At the designated times after injection, animals were anesthetized and then sacrificed by decapitation. The dissected organs and collected excretions were counted for radioactivity in a gamma counter (Compugamma, LKB Wallac, Turku, Finland), and values of the percentage of injected dose per gram (% ID/g) and % ID were calculated.

For pretargeting studies, mice were injected i.v. with 1.5×10^{-10} mol (12 μg, 222-444 kBq ^{125}I) of the bsMAb (molecular weight assumed to be M_r 77,000 Da) in 0.1 mL followed 25 or 41 hours later with an i.v. injection (0.1 mL) of ^{111}In-labeled IMP-241 (1.5×10^{-11} mol, 296 kBq). After the animals were anesthetized and sacrificed by decapitation (at the indicated time points), the dissected organs and collected excretions were counted for radioactivity as described above for the nonpretargeted studies.

Mouse dosimetry. Self-to-self doses for mouse organs were estimated based on medical internal radiation dose (29) using the biodistribution results of the labeled MAb and peptide. Using ^{125}I and ^{111}In as surrogates, dosimetric calculations were made for the corresponding therapeutic isotopes ^{131}I and ^{90}Y as described earlier (21). About the dose-limiting organ, which was either the red marrow (directly targeted L19-SIP) or the kidneys (pretargeted peptide-hapten), maximum activities to be injected per mouse were determined based on published human tolerance doses of $TD_{5/5}$ = 2.5 Gy for the red marrow and $TD_{50/5}$ = 20 Gy for the kidneys (30). These maximum tolerated activities per mouse were used to calculate absolute tumor doses (in Gy) for a 100 mg normalized tumor mass in relation to the respective dose-limiting organ (therapeutic index).

Results

Characterization of the AP39xm679 bsMAb. The affinity-purified preparation of AP39xm679 bsMAb was shown by size exclusion HPLC (Fig. 2A) to consist of a major peak at 8.89 minutes corresponding to the expected molecular size of ~75,000 Da, an ascending shoulder at 8.11 minutes, and a minor peak at 10.36 minutes. A buffer peak at 11.44 minutes was also observed. Surface plasmon analysis (BIAcore) indicated that the purified AP39xm679 contained binding specificities for both HSG and ED-B (Fig. 2B and C).

Radiolabeling of antibodies and HSG-hapten-peptide. The radiochemical yield of the radioiodinations ranged between 60% and 90%, and the radiochemical purity, as determined by size exclusion HPLC, was always >80% with <5% of free iodide. For all iodinated proteins, the immunoreactivity was >80%. The radiochemical purity of the ^{111}In-labeled hapten-peptide, as determined by instant TLC and reversed-phase HPLC, was always >90% with no free ^{111}In in the samples.

Downloaded from http://aacrjournals.org/clincancerres/article-pdf/12/18/5587/1966519/5587.pdf by guest on 10 November 2024

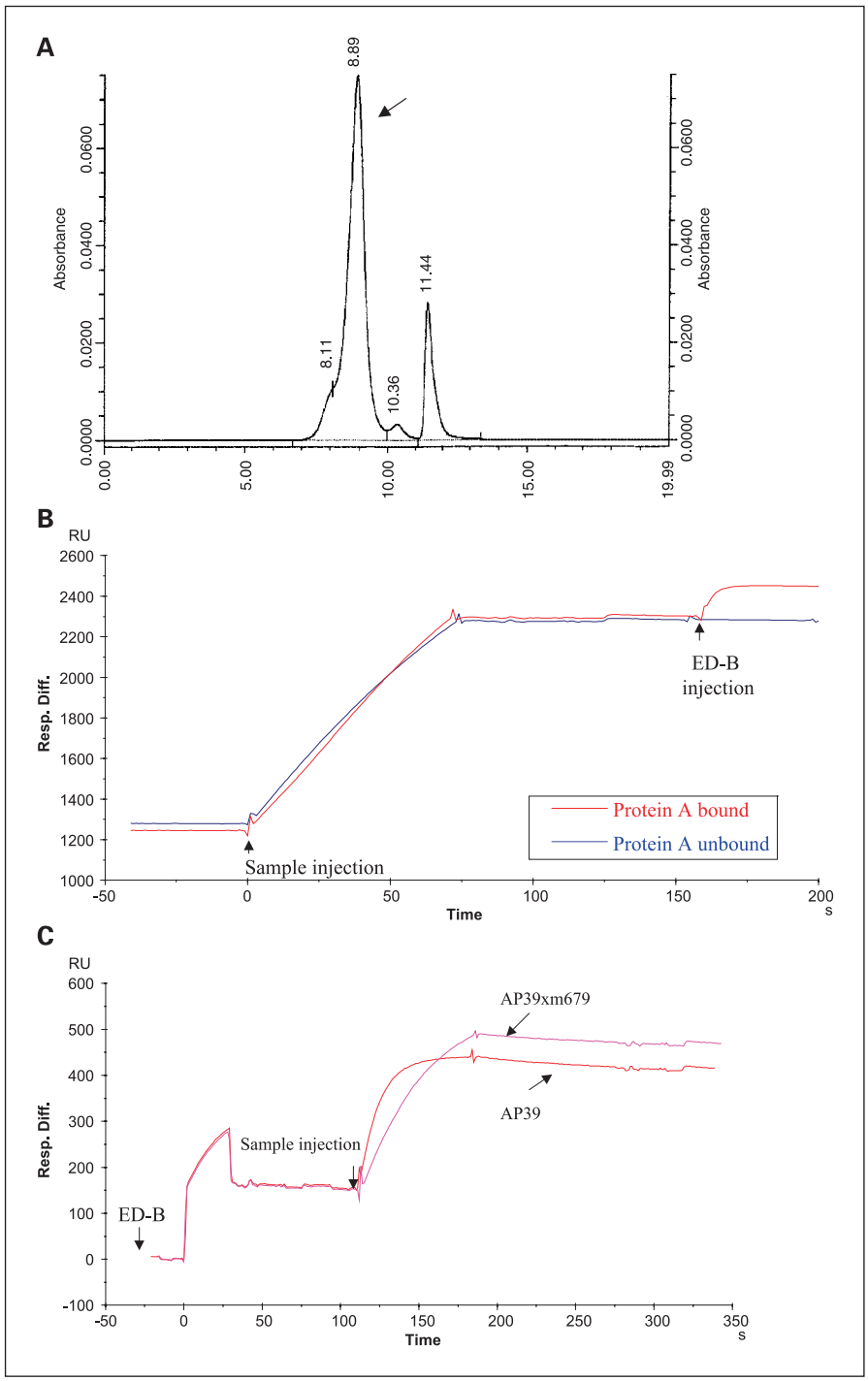

Fig. 2. Characterization of the AP39xm679 bsMAb. *A,* size exclusion HPLC of purified AP39xm679 bsMAb showing the product as a major peak with a molecular size of ~80 kDa. *B,* BIAcore analysis examining the binding of the bsMAb to a HSG-peptide chip. Once the material was bound, ED-B was injected to determine the presence of functional AP39. Although both the protein A – bound and flow-through fractions bound to the HSG chip, only the protein A – bound fraction was also able to bind ED-B, indicating bispecific-binding properties. *C,* ED-B was injected and allowed to bind to a Ni-NTA chip, and after a 90-second wash, either AP39xm679 bsMAb or AP39 scFv was injected. Both products had similar ED-B-binding properties.

Biodistribution of ^{125}I-labeled AP39xm679 bsMAb and L19-SIP in tumor-bearing mice. The biodistribution and pharmacokinetic data for the ^{125}I-labeled AP39xm679 bsMAb compared with the L19-SIP in tumor-bearing mice are shown in Tables 1 and 2 Both products cleared rapidly from the blood, with ~1.3% ID/g in the blood 1 day after their injection and with maximum tumor accumulation occurring at 4 hours after injection and with similar uptake (averaging between 17% and 20% ID/g) and retention. These data suggest that the bsMAb retained its ability to target ED-B as well as L19-SIP did, with similar pharmacokinetic properties.

The different specific activities of the radiolabels of the ^{125}I-AP39xm679 used for the initial investigation of biodistribution and for monitoring of the bsMAb in the pretargeting experiments did not significantly affect biodistribution and tumor uptake (data not shown).

AP39xm679-pretargeted ^{111}In-hapten-peptide. Previous experience with bsMAb pretargeting systems, including bsMAbs based on the 679 anti-HSG MAb, suggested that optimal pretargeting results can be obtained when (*a*) 10-fold more moles of the bsMAb are given compared with the moles of radiolabeled hapten-peptide to be injected, (*b*) the

Downloaded from http://aacrjournals.org/clincancerres/article-pdf/12/18/5587/1966519/5587.pdf by guest on 10 November 2024

Table 1. Biodistribution of ^{125}I-AP39xm679 in U251 tumor-bearing nude mice given in % ID/g

	Time after injection				
Tissue	**1 h**	**4 h**	**24 h**	**48 h**	**72 h**
Uptake in % ID/g					
Tumor	8.6 ± 1.8	16.8 ± 7.1	8.8 ± 0.5	9.3 ± 1.7	6.2 ± 2.0
Blood	20.3 ± 1.7	10.0 ± 1.0	1.4 ± 0.1	0.4 ± 0.0	0.2 ± 0.1
Spleen	5.3 ± 1.0	3.1 ± 0.4	0.7 ± 0.1	0.4 ± 0.1	0.2 ± 0.0
Liver	6.5 ± 1.1	3.9 ± 0.3	0.5 ± 0.0	0.2 ± 0.0	0.1 ± 0.0
Kidney	8.8 ± 2.1	6.8 ± 0.5	0.9 ± 0.1	0.4 ± 0.1	0.2 ± 0.0
Lung	9.4 ± 3.8	5.9 ± 1.3	1.1 ± 0.1	0.5 ± 0.1	0.2 ± 0.0
Bone	3.7 ± 0.9	3.5 ± 0.5	1.6 ± 0.5	0.9 ± 0.3	0.7 ± 0.2
Thyroid	6.1 ± 2.0	22.8 ± 5.2	233.0 ± 74.6	108.1 ± 67.1	249.6 ± 40.0
Muscle	0.5 ± 0.2	0.8 ± 0.2	0.3 ± 0.1	0.2 ± 0.0	0.1 ± 0.0
Ovary	16.0 ± 1.6	9.7 ± 1.5	8.5 ± 1.1	2.7 ± 1.2	2.8 ± 2.3
Uterus	3.4 ± 1.9	2.0 ± 0.8	4.3 ± 2.1	3.2 ± 2.2	1.8 ± 0.7
Excretion in % ID					
Urine	4.4 ± 0.8	9.0 ± 2.3	55.1 ± 4.2	62.6 ± 3.0	68.2 ± 4.1
Feces	0.0 ± 0.0	0.2 ± 0.3	7.1 ± 1.9	5.3 ± 3.0	5.0 ± 3.3

NOTE: Total excretion is measured cumulatively at indicated time points and is calculated as % ID. All data are presented as mean and SD (n = 3).

hapten-peptide should be radiolabeled at its highest specific activity, and (c) the blood concentration of the bsMAb should be ≤1.0% ID/g before the radiolabeled hapten-peptide is given (31). The blood clearance data for the ^{125}I-AP39xm679 bsMAb indicated that the ^{111}In-hapten-peptide should be given between 24 and 48 hours after the bsMAb injection (Table 1). Therefore, two different groups of mice were examined, one where the ^{111}In-hapten-peptide was given at 25 hours and the other at 41 hours. In both cases, the molar ratio of bsMAb to peptide was 10:1. Biodistributions in tumor-bearing mice were carried out up to 168 hours after injection of the radiolabeled hapten-peptide.

The tumor and tissue uptake and clearance for the pretargeted ^{111}In-hapten-peptide using the two intervals tested, along with the data for the ^{125}I-L19-SIP, are shown in Tables 2 and 3A and B as well as in Fig. 3. The variation of the clearance time did not affect biodistribution and tumor targeting of ^{111}In-hapten-peptide. Moreover, tumor uptake of the ^{111}In-hapten-peptide remained in the tumors at a more sustained level than that seen with the directly radiolabeled ^{125}I-L19-SIP (Tables 2 and 3A and B; Fig. 3A). The ^{111}In-hapten-peptide was efficiently cleared from the body through the urine, whereas only a small fraction was found in the feces (Tables 3A and B and 4).

In addition to the uptake seen in tumors, the ovaries and the uterus showed an increased uptake of pretargeted ^{111}In-hapten-peptide (Table 3A and B). Similarly, both the bsMAb and the L19-SIP showed an enhanced uptake in these tissues (Tables 1 and 2).

In contrast to pretargeting settings, the uptake of ^{111}In-hapten-peptide alone in tumor and normal tissue (including ovaries and uterus) was rather low (Table 4).

Table 2. Biodistribution of ^{125}I-L19-SIP in U251 tumor-bearing nude mice given in % ID/g

	Time after injection				
Tissue	**1 h**	**4 h**	**24 h**	**48 h**	**72 h**
Uptake in % ID/g					
Tumor	9.0 ± 3.2	20.3 ± 2.4	12.5 ± 3.6	9.9 ± 1.3	5.4 ± 1.5
Blood	17.8 ± 2.2	8.2 ± 0.8	1.3 ± 0.1	0.3 ± 0.0	0.2 ± 0.0
Spleen	3.5 ± 0.3	2.4 ± 0.4	0.6 ± 0.1	0.1 ± 0.0	0.1 ± 0.0
Liver	5.2 ± 0.4	2.4 ± 0.2	0.5 ± 0.0	0.1 ± 0.0	0.1 ± 0.0
Kidney	10.6 ± 2.3	5.5 ± 0.5	0.9 ± 0.3	0.3 ± 0.1	0.1 ± 0.1
Lung	8.5 ± 3.7	5.8 ± 0.7	1.3 ± 0.1	0.4 ± 0.0	0.2 ± 0.0
Bone	2.5 ± 0.3	3.5 ± 1.8	1.2 ± 0.3	0.5 ± 0.1	0.3 ± 0.1
Thyroid	8.7 ± 4.9	74.8 ± 61.6	242.9 ± 171.2	146.4 ± 120.2	130.1 ± 82.6
Muscle	0.9 ± 0.3	1.1 ± 0.1	0.2 ± 0.1	0.1 ± 0.0	0.1 ± 0.0
Ovary	10.2 ± 0.7	14.5 ± 5.0	3.1 ± 0.7	1.3 ± 0.2	1.0 ± 0.3
Uterus	3.4 ± 0.6	7.2 ± 1.0	7.9 ± 4.4	2.5 ± 0.3	2.8 ± 1.3
Excretion in % ID					
Urine	1.5 ± 0.4	11.2 ± 3.9	56.2 ± 2.5	72.6 ± 3.7	74.0 ± 8.3
Feces	0.0 ± 0.0	0.1 ± 0.2	3.4 ± 1.0	3.3 ± 0.1	3.0 ± 1.0

NOTE: Total excretion is measured cumulatively at indicated time points and is calculated as % ID. All data are presented as mean and SD (n = 3).

Downloaded from http://aacrjournals.org/clincancerres/article-pdf/12/18/5587/1966519/5587.pdf by guest on 10 November 2024

Dosimetry calculations. Based on the results from the biodistribution experiments with AP39xm679-pretargeted ^{111}In-hapten-peptide and ^{125}I-L19-SIP, the self-to-self organ doses in mice were estimated for the respective therapeutic radioisotopes ^{90}Y and ^{131}I, respectively. The highest calculated dose levels can be observed in tumor as well as in ovaries and uterus. Pretargeting the tumors with AP39xm679 using either a 25-hour or a 41-hour clearance time yielded a much higher radiation dose to the tumors if compared with the directly targeted L19-SIP (2,568 and 2,278 mGy/MBq for the 25-hour and 41-hour clearance times, respectively, versus 939 mGy/MBq for L19-SIP). The increased dose levels in both uterus and ovaries are consistent with known ED-B expression in these organs (32). The radiation doses for the other investigated tissues and organs were comparable in the pretargeting and the directly radiolabeled L19-SIP groups (data not shown).

In contrast to ^{131}I-L19-SIP, where the red marrow was the dose-limiting organ when related to the human tolerance dose ($TD_{5/5}$ = 2.5 Gy), for the pretargeted ^{90}Y-hapten-peptide the kidneys were the dose-limiting organ ($TD_{5/5}$ = 20 Gy). It was calculated that 59 MBq (25-hour clearance interval) and 57 MBq (41-hour clearance interval) of AP39xm679-pretargeted ^{90}Y-hapten-peptide could be injected per mouse to achieve this maximally tolerated kidney dose (Fig. 4). This maximum tolerable activity would result in a tumor dose of 146 and 134 Gy, respectively. For ^{131}I-L19-SIP, the corresponding maximum tolerable activity per mouse was 48 MBq, resulting in a tumor dose of 45 Gy (Fig. 4). The ratio between the U251 tumor (100 mg) and the dose-limiting organ was defined as the therapeutic index and was higher for ^{131}I-L19-SIP (index value, 18) if compared with the AP39xm679-pretargeted ^{90}Y-hapten-peptide (index value, ~7 for both investigated clearance intervals).

Discussion

In this report, the radiotherapeutic potential of two different techniques, (*a*) direct targeting of the radioiodinated, divalent L19-SIP and (*b*) a two-step pretargeting method, was compared in a human glioblastoma xenograft mouse model. Both MAb constructs target ED-B fibronectin, a stromal tumor marker strongly associated with neovascularization. A novel bsMAb pretargeting system that uses an anti-HSG-HSG-peptide secondary recognition system was used because this is highly flexible and has the potential to target a variety of compounds (28).

Downloaded from http://aacrjournals.org/clincancerres/article-pdf/12/18/5587/1966519/5587.pdf by guest on 10 November 2024

Table 3. Biodistribution of ^{111}In-IMP-241 in U251 tumor-bearing nude mice after 25-hour (A) and 41-hour (B) clearance time of bsMab

A. Time after injection of ^{111}In-IMP-241

Tissue	4 h	24 h	48 h	120 h	168 h
Uptake in % ID/g					
Tumor	13.5 ± 2.5	16.7 ± 1.2	13.1 ± 0.5	10.2 ± 0.7	5.6 ± 0.9
Blood	0.5 ± 0.1	0.2 ± 0.0	0.1 ± 0.0	0.1 ± 0.0	0.0 ± 0.0
Spleen	0.7 ± 0.2	0.5 ± 0.1	1.3 ± 1.6	0.8 ± 1.0	1.6 ± 2.2
Liver	0.5 ± 0.1	0.4 ± 0.1	0.3 ± 0.1	0.2 ± 0.0	0.2 ± 0.0
Kidney	1.4 ± 0.2	1.1 ± 0.3	0.7 ± 0.1	0.7 ± 0.2	0.2 ± 0.0
Lung	1.0 ± 0.2	0.6 ± 0.1	0.4 ± 0.1	0.3 ± 0.1	0.1 ± 0.1
Bone	4.1 ± 0.5	3.9 ± 0.2	3.4 ± 0.8	2.0 ± 0.1	1.3 ± 0.3
Thyroid	3.0 ± 0.7	3.0 ± 0.5	2.6 ± 0.9	1.8 ± 0.4	1.5 ± 0.5
Muscle	0.3 ± 0.1	0.2 ± 0.0	0.1 ± 0.1	0.1 ± 0.0	0.1 ± 0.0
Ovary	10.2 ± 3.6	6.6 ± 2.2	7.9 ± 2.1	9.7 ± 4.9	4.6 ± 2.1
Uterus	9.5 ± 5.8	8.4 ± 2.7	16.1 ± 4.8	10.3 ± 2.4	10.1 ± 1.8
Excretion in % ID					
Urine	44.5 ± 1.9	53.2 ± 3.1	63.3 ± 3.9	65.9 ± 7.8	86.7 ± 2.2
Feces	2.3 ± 3.9	1.6 ± 0.5	2.7 ± 0.6	3.6 ± 1.1	4.5 ± 1.4

B. Time after injection of ^{111}In-IMP-241

Tissue	4 h	24 h	48 h	120 h	168 h
Uptake in % ID/g					
Tumor	16.9 ± 3.6	10.6 ± 1.1	10.1 ± 2.4	8.7 ± 0.9	7.6 ± 1.6
Blood	0.3 ± 0.1	0.1 ± 0.0	0.1 ± 0.0	0.0 ± 0.0	0.0 ± 0.0
Spleen	0.3 ± 0.1	0.2 ± 0.0	0.3 ± 0.1	0.5 ± 0.1	1.1 ± 1.2
Liver	0.3 ± 0.1	0.2 ± 0.0	0.2 ± 0.0	0.2 ± 0.0	0.1 ± 0.1
Kidney	1.5 ± 0.2	1.0 ± 0.1	0.8 ± 0.1	0.5 ± 0.1	0.3 ± 0.1
Lung	0.6 ± 0.2	0.3 ± 0.1	0.2 ± 0.0	0.2 ± 0.0	0.2 ± 0.1
Bone	3.0 ± 0.7	2.4 ± 0.4	2.0 ± 0.4	1.1 ± 0.4	0.7 ± 0.1
Thyroid	2.4 ± 1.0	1.7 ± 0.8	2.1 ± 1.2	1.1 ± 0.5	1.0 ± 0.0
Muscle	0.2 ± 0.0	0.1 ± 0.0	0.1 ± 0.0	0.1 ± 0.0	0.1 ± 0.0
Ovary	7.0 ± 5.7	5.4 ± 2.5	3.4 ± 0.9	4.4 ± 1.3	3.9 ± 2.2
Uterus	13.8 ± 1.0	13.4 ± 6.4	10.1 ± 3.1	12.2 ± 5.9	15.5 ± 12.3
Excretion in % ID					
Urine	73.3 ± 4.3	76.5 ± 1.6	82.7 ± 2.5	78.6 ± 10.0	92.1 ± 0.2
Feces	0.0 ± 0.0	1.8 ± 1.0	0.9 ± 0.1	2.0 ± 0.9	6.0 ± 3.9

NOTE: Biodistribution is given in % ID/g. Total excretion is measured cumulatively at indicated time points and is calculated as % ID. Time points are indicated as hours after injection of ^{111}In-IMP-241. All data are presented as mean and SD (n = 3).

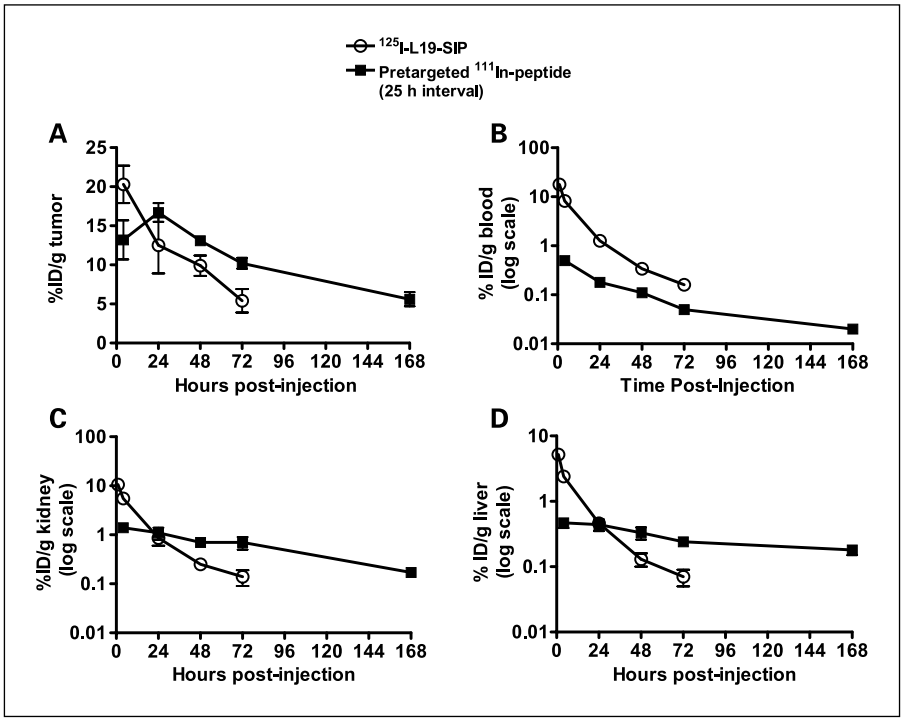

Fig. 3. Biodistribution and tumor targeting of pretargeted ^{111}In peptide and ^{125}I-L19-SIP in nude mice bearing U251 human glioblastoma tumors. Data (% ID/g) for tumor (*A*), blood (*B*), kidneys (*C*), and liver (*D*). Points, mean (n = 3); bars, SD.

Because bsMAb can be fully humanized, these pretargeting agents would be less immunogenic than those using streptavidin. In most instances reported in the literature, bsMAbs are commonly prepared from Fabs or IgGs, but our results clearly indicate that chemical combinations of a Fab′ and a modified scFv (using an additional unpaired cysteine residue) can lead to the efficient generation of a functional bsMAb. Importantly, this bsMAb showed high tumor retention over a 3-day period, while at the same time quickly clearing from the blood and nontumor tissues. Good tumor retention and the fast blood clearance are highly favorable properties for a bsMAb to be used as a pretargeting tool.

^{111}In-labeled HSG-peptide, when used for pretargeting, showed a rapid and high (~17% ID/g) tumor uptake that rivaled that of the ^{125}I-labeled L19-SIP, but tumor retention was longer with the pretargeted peptide. The enhanced retention most likely reflects the use of a radiometal-labeled pretargeted peptide, whereas the directly radiolabeled MAb was radioiodinated. Radiometal-labeled MAbs frequently have a longer retention in tumors than radioiodinated forms because radioiodinated MAbs can be dehalogenated, or when internalized and catabolized, radioiodine will be quickly eliminated from the cell, whereas radiometals are retained (33). ^{131}I-L19-SIP was used because earlier studies had indicated that renal uptake of ^{111}In-L19-SIP was ~2-fold higher than tumor uptake for this agent, with dosimetry data indicating unfavorable tumor-to-kidney ratios for ^{90}Y-L19-SIP (21). Thus, ^{131}I-L19-SIP was found to be the best therapeutic agent compared with ^{111}In-L19-SIP and two other L19 MAb formats radiolabeled with ^{131}I or ^{111}In/^{90}Y. In contrast, the pretargeting procedure used in this study has the advantage of being receptive to a variety of radionuclides, having been studied already with ^{131}I, ^{99m}Tc, ^{111}In, ^{90}Y, and ^{177}Lu (8, 28, 34), and in each instance, excellent tumor-to-nontumor ratios, even tumor-to-kidney ratios, were reported.

Previous studies suggested that the concentration of bsMAb in the blood needed to be ≤1.0% ID/g to facilitate optimal pretargeting (31). Therefore, we investigated two different clearance intervals in the U251 tumor model, 25 and 41 hours, which, based on the clearance of the AP39xm679 bsMAb, suggested blood concentrations of approximately 1.4% and 0.4% ID/g (i.e., at 24 and 48 hours, respectively). Regardless of the interval at which the ^{111}In-hapten-peptide was given, tumor uptake and the total amount of radioactivity delivered to the tumor at an estimated maximum tolerated dose were similar.

Table 4. Biodistribution of ^{111}In-IMP-241 alone in U251 tumor-bearing nude mice given in % ID/g

Tissue	Time after injection		
	0.5 h	3 h	24 h
Uptake in % ID/g			
Tumor	0.8 ± 0.1	0.1 ± 0.0	0.0 ± 0.0
Blood	0.5 ± 0.1	0.0 ± 0.0	0.0 ± 0.0
Spleen	0.2 ± 0.0	0.1 ± 0.0	0.0 ± 0.0
Liver	0.2 ± 0.0	0.1 ± 0.0	0.1 ± 0.0
Kidney	3.6 ± 0.7	2.1 ± 0.3	0.9 ± 0.1
Lung	0.7 ± 0.2	0.1 ± 0.0	0.0 ± 0.0
Bone	0.2 ± 0.0	0.0 ± 0.0	0.0 ± 0.0
Thyroid	0.4 ± 0.1	0.3 ± 0.1	0.1 ± 0.0
Muscle	0.1 ± 0.0	0.0 ± 0.0	0.0 ± 0.0
Ovary	0.3 ± 0.0	0.1 ± 0.0	0.1 ± 0.0
Uterus	0.4 ± 0.1	0.1 ± 0.0	0.1 ± 0.0
Excretion in % ID			
Urine	93.4 ± 3.3	92.7 ± 9.8	97.9 ± 2.7
Feces	—	3.2 ± 4.9	0.3 ± 0.0

NOTE: Total excretion is measured cumulatively at indicated time points and is calculated as % ID. All data are presented as mean and SD (n = 3).

Downloaded from http://aacrjournals.org/clincancerres/article-pdf/12/18/5587/1966519/5587.pdf by guest on 10 November 2024

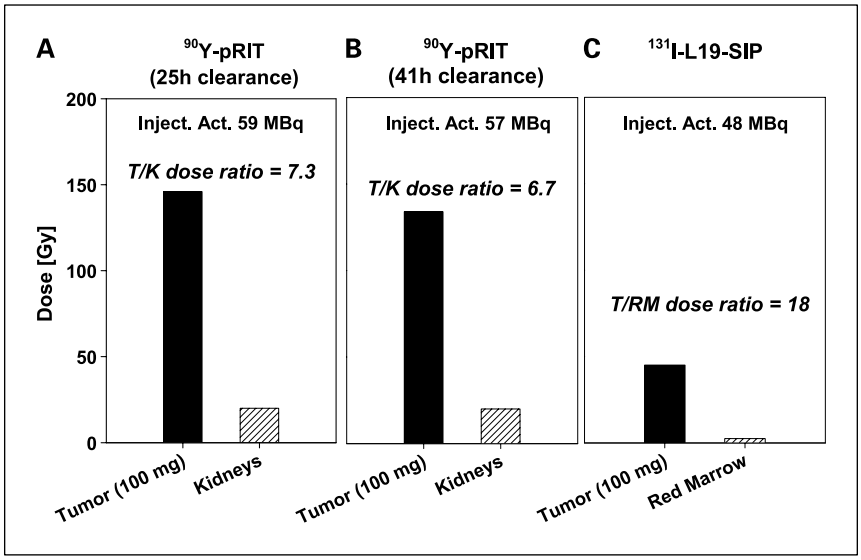

Fig. 4. Depiction of the U251 tumor and organ doses (Gy). The therapeutic index was calculated as tumor to organ dose ratio and maximum tolerated dose (MBq) for AP39xm679-pretargeted ^{90}Y peptide after 25 hours (*A*) and 41 hours of bsMAb clearance (*B*) as well as for ^{131}I-L19-SIP (*C*). For each particular radioimmunoconjugate, the dose delivery is shown for the respective dose-limiting organ (at $TD_{5/5}$) and for a tumor mass of 100 mg.

This most likely reflected the relative stability of this bsMAb in the tumor at these two intervals, allowing for the optimal capture of the bsMAb in the tumor, whereas the bsMAb concentration in the blood was sufficiently low, even at 25 hours, to allow the peptide to clear from the blood relatively unabated.

In addition, there was also high uptake in several normal tissues, such as the uterus and ovaries. This targeting of radioactivity to uterus and ovary is consistent with the described ED-B expression in these organs (32). However, polyovulation in mouse ovaries is not comparable with the human situation and is therefore not considered a dose-limiting organ.

The use of medical internal radiation dose software-based calculations of radiodosimetry from biodistribution experiments is widely used to estimate the radiation doses delivered to different organs of interest. However, dosimetry based on medical internal radiation dose is limited because it uses several simplified assumptions, such as homogenous organ and tumor distribution of labeled compounds (29). Nevertheless, Berndorff et al. (21) showed the predictive power and the applicability of medical internal radiation dose dosimetry calculations in a tumor model by targeting ED-B fibronectin with different radiolabeled immunoconjugates (L19 scFv, L19-SIP, and L19-IgG) and were able to confirm the dose-limiting organ and corresponding maximum tolerated dose predicted by medical internal radiation dose based on myelotoxicity studies. According to this procedure, we identified the kidney as the dose-limiting organ as well as the corresponding maximum tolerated dose for AP39xm679-pretargeted ^{90}Y-hapten-peptide. In accordance, Karacay et al. (13) recently showed that, in a similar pretargeting system using a ^{90}Y-labeled peptide, renal toxicity was dose limiting. In our pretargeting approach, the calculated tumor dose at $TD_{5/5}$ for AP39xm679-pretargeted ^{90}Y-hapten-peptide was 146 Gy, which is 3-fold greater when compared with the $TD_{5/5}$ tumor dose of the directly targeted ^{131}I-L19-SIP (45 Gy). It should also be noted that ^{90}Y has a greater energy emission than ^{131}I (β; E_{max} = 2.27 MeV versus β; E_{max} = 0.81 MeV, respectively) and a shorter half-life ($t_{1/2}$ = 2.67 days versus $t_{1/2}$ = 8.06 days, respectively). In addition, ^{90}Y will deposit its energy out to 1.81 cm versus only 0.55 cm for ^{131}I (35), thus making it a more desirable radionuclide for the treatment of solid tumors. In fact, when directly compared at equal radiation doses delivered to a human pancreatic adenocarcinoma in mice, ^{90}Y was shown to be superior to ^{131}I in terms of therapeutic efficacy of these solid tumors (36).

In the current investigation, the advantage of pretargeting becomes most obvious when compared with ^{111}In-labeled L19-SIP, which has been investigated in F9 teratocarcinoma-bearing mice (21). We have observed that ED-B-based targeting in the F9 tumor model is comparable with the U251 tumor model (data not shown). However, at the $TD_{5/5}$, ^{90}Y-labeled L19-SIP delivers only 7 Gy of ^{90}Y to the F9 tumor, whereas in the current investigation we showed that, by using AP39xm679 pretargeting, a 21-fold higher ^{90}Y radiation dose to the U251 tumor could be achieved (i.e., 146 Gy). It seems that pretargeted radioimmunotherapy would be superior for the treatment of ED-B-expressing solid tumors when compared with ^{131}I-L19-SIP, which was previously identified as the best-suited, directly labeled, immunoconjugate for radiotherapy (21).

In conclusion, we have shown that an AP39xm679 bsMAb platform to pretarget a subsequently given radiolabeled hapten-peptide to ED-B-expressing tumors is substantially superior to using a directly radiolabeled anti-ED-B L19-SIP. These data clearly indicate that this pretargeting system with a ^{90}Y-labeled hapten-peptide, with its advantageous properties (e.g., long-range radiation and cross-fire effect), is a solid basis for developing future strategies for pretargeted radioimmunotherapy of solid tumors.

Acknowledgments

We thank Melanie Appel, Guel Caglar, Joerg Pioch, Volker Stickel, Ingolf Weber, and Simone Zolchow for excellent technical assistance with regard to the radiolabeling, cell culture, and biodistribution studies; John Kopinski and Li Zeng for help in the preparation and characterization of the bispecific conjugates; and Dr. Guido Malawski for purification of scFv AP39.

Downloaded from http://aacrjournals.org/clincancerres/article-pdf/12/18/5587/1966519/5587.pdf by guest on 10 November 2024

References

1. Sharkey RM, Goldenberg DM. Perspectives on cancer therapy with radiolabeled monoclonal antibodies. J Nucl Med 2005;46 Suppl 1:115–27s.

2. Sharkey RM, Blumenthal RD, Hansen HJ, Goldenberg DM. Biological considerations for radioimmunotherapy. Cancer Res 1990;50:964–9s.

3. Behr TM, Becker WS, Sharkey RM, et al. Reduction of renal uptake of monoclonal Ab fragments by amino acid infusion. J Nucl Med 1996;37:829–33.

4. Chang CH, Sharkey RM, Rossi EA, et al. Molecular advances in pretargeting radioimmunotherapy with bispecific antibodies. Mol Cancer Ther 2002;1: 553–63.

5. Boerman OC, van Schaijk FG, Oyen WJ, Corstens FH. Pretargeted radioimmunotherapy of cancer: progress step by step. J Nucl Med 2003;44:400–11.

6. Sharkey RM, Karacay H, Cardillo TM, et al. Improving the delivery of radionuclides for imaging and therapy of cancer using pretargeting methods. Clin Cancer Res 2005;11:7109–21.

7. Le Doussal JM, Martin M, Gautherot E, Delaage M, Barbet J. *In vitro* and *in vivo* targeting of radiolabeled monovalent and divalent haptens with dual specificity monoclonal Ab conjugates: enhanced divalent hapten affinity for cell-bound antibody conjugate. J Nucl Med 1989;30:1358–66.

8. Gautherot E, Rouvier E, Daniel L, et al. Pretargeted radioimmunotherapy of human colorectal xenografts with bispecific antibody and ^{131}I-labeled bivalent hapten. J Nucl Med 2000;41:480–7.

9. Axworthy DB, Reno JM, Hylarides MD, et al. Cure of human carcinoma xenografts by a single dose of pretargeted yttrium-90 with negligible toxicity. Proc Natl Acad Sci U S A 2000;97:1802–7.

10. Yao Z, Zhang M, Axworthy DB, et al. Radioimmunotherapy of A431 xenografted mice with pretargeted B3 antibody-streptavidin and ^{90}Y-labeled 1,4,7,10-tetraazacyclododecane-*N*,*N*′,*N*″,*N*‴-tetraacetic acid (DOTA)-biotin. Cancer Res 2002;62: 5755–60.

11. Subbiah K, Hamlin DK, Pagel JM, et al. Comparison of immunoscintigraphy, efficacy, and toxicity of conventional and pretargeted radioimmunotherapy in CD20-expressing human lymphoma xenografts. J Nucl Med 2003;44:437–45.

12. Sharkey RM, Karacay H, Chang CH, et al. Improved therapy of non-Hodgkin's lymphoma xenografts using radionuclides pretargeted with a new anti-CD20 bispecific antibody. Leukemia 2005;19:1064–9.

13. Karacay H, Brard P-Y, Sharkey RM, et al. Therapeutic advantage of pretargeted radioimmunotherapy using a recombinant bispecific antibody in a human colon cancer xenograft. Clin Cancer Res 2005;11:7879–85.

14. Kraeber-Bodere F, Sai-Maurel C, Campion L, et al. Enhanced antitumor activity of combined pretargeted radioimmunotherapy and paclitaxel in medullary thyroid cancer xenografts. Mol Cancer Ther 2002; 1:267–74.

15. Castellani P, Viale G, Dorcaratto A, et al. The fibronectin containing the ED-B oncofetal domain: a marker of angiogenesis. Int J Cancer 1994;59:612–8.

16. Pini A, Viti F, Santucci A, et al. Design and use of a phage display library. Human antibodies with subnanomolar affinity against a marker of angiogenesis eluted from a two-dimensional gel. J Biol Chem 1998; 273:21769–76.

17. Tarli L, Balza E, Viti F, et al. A high-affinity human antibody fragment that targets tumoral blood vessels. Blood 1999;94:192–8.

18. Nilsson F, Kosmehl H, Zardi L, Neri D. Targeted delivery of tissue factor to the ED-B domain of fibronectin, a marker of angiogenesis, mediates the infarction of solid tumors in mice. Cancer Res 2001;61:711–6.

19. Carnemolla B, Borsi L, Balza E, et al. Enhancement of the antitumor properties of interleukin-2 by its targeted delivery to the tumor blood vessel extracellular matrix. Blood 2002;99:1659–65.

20. Santimaria M, Moscatelli G, Viale GL, et al. Immunoscintigraphic detection of the ED-B domain of fibronectin, a marker of angiogenesis, in patients with cancer. Clin Cancer Res 2003;9:571–9.

21. Berndorff D, Borkowski S, Sieger S, et al. Radioimmunotherapy of solid tumors by targeting extra domain B fibronectin: identification of the best-suited radioimmunoconjugate. Clin Cancer Res 2005;11: 7053–63.

22. Cunha AE, Clemente JJ, Gomes R, et al. Methanol induction optimization for scFv antibody fragment production in *Pichia pastoris*. Biotechnol Bioeng 2004;86:458–67.

23. Borsi L, Balza E, Bestagno M, et al. Selective targeting of tumoral vasculature: comparison of different formats of an antibody (L19) to the ED-B domain of fibronectin. Int J Cancer 2002;102:75–85.

24. Scheuermann J, Viti F, Neri D. Unexpected observation of concentration-dependent dissociation rates for antibody-antigen complexes and other macromolecular complexes in competition experiments. J Immunol Methods 2003;276:129–34.

25. Rossi EA, Chang C-H, Losman MJ, et al. Pretargeting of CEA-expressing cancers with a trivalent bispecific fusion protein produced in myeloma cells. Clin Cancer Res 2005;11:7122–9.

26. Fraker PJ, Speck JC. Protein and cell membrane iodinations with a sparingly soluble chloramide 1,3,4,6-tetrachloro-3α-6α-diphenylglycouril. Biochem Biophys Res Commun 1978;80:849–57.

27. Birchler M, Neri G, Tarli L, Halin C, Viti F, Neri D. Infrared photodetection for the *in vivo* localization of phage-derived antibodies directed against angiogenic markers. J Immunol Methods 1999;231:239–48.

28. Sharkey RM, McBride WJ, Karacay H, et al. A universal pretargeting system for cancer detection and therapy using bispecific antibody. Cancer Res 2003; 63:354–63.

29. Loevinger R, Budinger T, Watson E. MIRD primer for absorbed dose calculations. New York: Society of Nuclear Medicine; 1988.

30. Pizarello DJ, Witcofski RL. Medical radiation biology. Philadelphia: Lea & Febiger; 1982.

31. Sharkey RM, Karacay H, Richel H, et al. Optimizing bispecific antibody pretargeting for use in radioimmunotherapy. Clin Cancer Res 2003;9:3897–913S.

32. Carnemolla B, Balza E, Siri A, et al. A tumor-associated fibronectin isoform generated by alternative splicing of messenger RNA precursors. J Cell Biol 1989;108:1139–48.

33. Vangeepuram N, Ong GL, Mattes MJ. Processing of antibodies bound to B-cell lymphomas and lymphoblastoid cell lines. Cancer 1997;80:2425–30.

34. Sharkey RM, Cardillo TM, Rossi EA, et al. Signal amplification in molecular imaging by pretargeting a multivalent bispecific antibody. Nature Medicine 2005;11:1250–5.

35. Bureau of Radiological Health. Radiological health handbook. Revised ed. Jan. 1970. Rockville (MD): U.S. Department of Health, Education, and Welfare.

36. Cardillo TM, Ying Z, Gold DV. Therapeutic advantage of ^{90}Y- versus ^{131}I-labeled PAM4 antibody in experimental pancreatic cancer. Clin Cancer Res 2001;7: 3186–92.

Downloaded from http://aacrjournals.org/clincancerres/article-pdf/12/18/5587/1966519/5587.pdf by guest on 10 November 2024